



# CHORUS

This is the accepted manuscript made available via CHORUS. The article has been published as:

## On the equivalence of nonequilibrium and equilibrium measurements of slip in molecular dynamics simulations

N. G. Hadjiconstantinou and M. M. Swisher

Phys. Rev. Fluids **7**, 114203 — Published 28 November 2022

DOI: [10.1103/PhysRevFluids.7.114203](https://doi.org/10.1103/PhysRevFluids.7.114203)

# Are non-equilibrium and equilibrium measurements of slip in molecular dynamics simulations equivalent?

N. G. Hadjiconstantinou and M. M. Swisher  
Department of Mechanical Engineering  
Massachusetts Institute of Technology  
Cambridge, MA 02139, USA

November 9, 2022

## Abstract

We show that non-equilibrium and equilibrium measurements of slip are consistent, provided the hydrodynamic wall location associated with the equilibrium measurement is properly taken into account. The latter is a strong function of the fluid state and wall-fluid interaction and cannot be neglected as it typically has. Our results are based on an alternative approach for calculating the hydrodynamic wall location which alleviates most of the difficulties associated with its calculation via a Green-Kubo integral that appear to have contributed to its neglect. Extensive molecular dynamics simulations are used to validate our approach including a model for calculating the slip length that does not involve a Green-Kubo integral.

## 1 Introduction

The hydrodynamic behavior of fluids under confinement is a topic of significant theoretical and practical importance. In many instances, slip/jump boundary conditions can be used [1, 2, 3] to extend the range of validity of traditional macroscopic hydrodynamic models into the regime of small, or in some cases even moderate confinement. The most well-known boundary condition of this type is, perhaps, the Navier slip boundary condition

$$u_x|_{z=z_w} = \beta \frac{\partial u_x}{\partial z}|_{z=z_w} \quad (1)$$

given here for a fluid-solid boundary, parallel to the  $z=0$  plane and located at  $z = z_w$ . We have also assumed, without loss of generality, that the solid boundary, or wall, is at rest and that the fluid flow and resulting slip is in the  $x$  direction.

Reliable methods for calculating the slip length  $\beta$  using molecular dynamics (MD) simulations are invaluable both from a practical point of view but also for informing fundamental research [4, 5, 6, 7, 8, 9, 10, 11] into relation (1) based on a microscopic description of the fluid-solid interaction at their interface. Slip in MD simulations can be measured in the presence of a velocity gradient by extrapolating the velocity profile to the wall location.

This approach is referred to as the non-equilibrium method. The inherent presence of non-equilibrium is considered to be a disadvantage by some authors, since, if the deviation from equilibrium is large, viscous heating, associated thermostats or other non-linear effects may contaminate the result. In response to this school of thought, methods for measuring slip using equilibrium simulations have also been developed. The most well-known, perhaps, is the Green-Kubo method proposed by Bocquet and Barrat [5], which invokes linear response theory to calculate  $\beta$ . More recently, Duque-Zumajo et al. [12] developed an alternative approach which avoids the well-known plateau problem associated with the Green-Kubo formulation [12, 13, 14]. Interestingly, in one of their publications [13] they are able to show that their GK expressions, although different in appearance, are equivalent to the original result of Bocquet and Barrat. Here we also note the work by Hansen et al. [15] who first introduced the concept of the near-wall fluid-slab on which the analysis by Duque-Zumajo et al. is based.

Given the existence of these two quite different approaches to measuring slip in MD simulations, the lack of a comprehensive investigation into their equivalence is conspicuous by its absence. Comparisons between the two methods have been brief and cursory, typically limited to the case of large slip length, with the hydrodynamic wall location, an important parameter within the GK method, neglected. On the other hand, typical modern computational resources are sufficient for performing low statistical uncertainty [16] non-equilibrium simulations at small deviations from equilibrium such that non-linear effects are negligible. In this work we undertake this task, namely a detailed comparison between non-equilibrium and Green-Kubo measurements of slip to show that the two approaches are indeed equivalent, provided the hydrodynamic wall location is properly taken into account. To this effect we propose a new approach for determining the latter quantity. Additionally, by partially evaluating the GK relation for the slip length developed by Bocquet and Barrat, we develop a model for calculating the slip length that does not involve a Green-Kubo integral.

## 2 Hydrodynamic wall location via tangential force balance at the wall

We consider an atomic liquid in contact with an atomically smooth solid. Let  $z$  denote the direction normal to the solid-liquid interface and pointing into the liquid, with  $z = 0$  corresponding to the first layer of solid atoms in contact with the liquid.

According to the Green-Kubo theory of Bocquet and Barrat [5], the slip length appearing in eq. (1) can be calculated from

$$\beta_{GK} = \frac{\mu A k_B T}{\int_0^\infty \langle F_x(t) F_x(0) \rangle dt}. \quad (2)$$

In this expression, angled brackets denote ensemble average,  $A$  denotes the interface area,  $k_B$  is Boltzmann's constant,  $\mu$  is the fluid viscosity and  $T$  is the (interface) temperature. Moreover  $F_x(t)$  denotes the force exerted by the solid on to the fluid in the  $x$  (slip) direction. According to this theory, the "hydrodynamic wall location" at which relation (1) is to be applied is not the fluid-solid interface ( $z = 0$ ), but a location inside the fluid given by

$$z_{GK}^w = \frac{\int_0^\infty \langle F_x(t) \Pi_{xz}(0) \rangle dt}{\int_0^\infty \langle F_x(t) F_x(0) \rangle dt} \quad (3)$$

where  $\Pi_{xz} = \sum_i m_i v_{xi} v_{zi} + \sum f_{xi} z_i$  denotes the  $x - z$  component of the fluid stress tensor,  $v_{ji}$  denotes the velocity of atom  $i$  in direction  $j$  and  $m_i$  denotes the mass of atom  $i$ ;  $i$  runs through all liquid atoms. Here we note that  $f_{xi}$ , the  $x$ -direction component of the force on liquid atom  $i$  includes the forces exerted by the solid onto the liquid.

A well-known issue [5] that limits the accuracy of GK approaches in finite systems (MD simulations) is associated with the identification of the "plateau" in integrals such as  $\int_0^\infty \langle F_x(t) F_x(0) \rangle dt$ . As remarked above, Dugue-Zumajo et al. have recently proposed [14] a reformulation that avoids these theoretical difficulties. On the other hand, researchers using eq (2) typically sidestep this issue by approximating [5] the plateau with the first peak of  $\int_0^t \langle F_x(t') F_x(0) \rangle dt'$ . Oga et al. [17] have recently provided some supporting argumentation for this approach by developing a model for the time evolution of  $\langle F_x(t) F_x(0) \rangle$  which reduces calculation of the autocorrelation integral to the determination of three fitting coefficients in the model. *Assuming their model to provide an accurate estimate of the GK integral*, they show that the error incurred by calculating  $\beta_{GK}$  using the first peak of the function  $\int_0^t \langle F_x(t') F_x(0) \rangle dt'$  becomes small when the separation between the viscoelastic and GK relaxation timescales in the system studied is large; moreover, according to their model, for typical values of these timescales found in MD simulations the discrepancy is on the order of a few percent. Our MD results (see figure 1) are consistent with these findings; namely, identifying the plateau with the first peak of  $\int_0^t \langle F_x(t') F_x(0) \rangle dt'$  results in a small over-estimation of  $\beta_{GK}$  of order 5% compared to the value predicted by the model of Oga et al.

Evaluation of expression (3) is more challenging. In addition to being significantly more sensitive to noise [5] than (2), a reliable approach for identifying the plateau in the additional GK integral has yet to be developed. As a result, the hydrodynamic wall location has received considerably less attention, with studies utilizing the GK formulation simply ignoring its existence or perhaps implicitly assuming that it is small compared to the slip length. Unfortunately, as will be seen below, the latter is not an appropriate assumption, even in the case of moderately large slip length. This can perhaps be used to explain the existence of a number of publications questioning the validity of (2); the reader is referred to Ref. [12] for a more thorough review of this body of work.

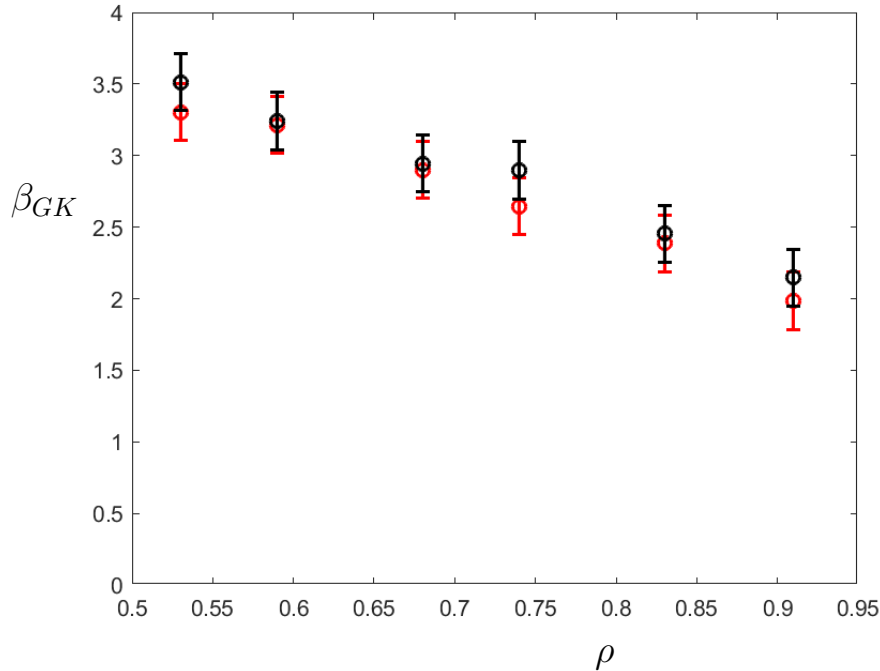


Figure 1: Comparison between estimates of  $\beta_{GK}$  calculated using the model of Oga et al. [17] (red) and by identifying the plateau by the first maximum of the running integral  $\int_0^t \langle F_x(t') F_x(0) \rangle dt'$  (black). Simulations performed at  $T = 1.5$  for  $\varepsilon_{sl} = 1$  and  $C_{sl} = 0.6$ .

Our objective here is to perform a thorough validation of the GK approach by comparing its predictions to non-equilibrium measurements of slip. To achieve this goal we need accurate measurements of the hydrodynamic wall location. We obtain those by using the tangential force balance at the wall [5]

$$\langle F_x \rangle = -\mu A \frac{u_x(z = z_{GK}^w)}{\beta_{GK}} \quad (4)$$

This serves as an implicit equation for  $z_{GK}^w$ , since the slip velocity  $u_x(z = z_{GK}^w)$  involves the (hydrodynamic) wall location in its definition. In other words, given a measurement of the force on the solid boundary,  $z_{GK}^w$  can be determined as the location at which  $u_x(z = z_{GK}^w)$  satisfies the above equation, with  $\beta_{GK}$  determined from eq. (2).

### 3 Validation

We have performed equilibrium and non-equilibrium MD simulations of a model system over a variety of conditions in order to (a) validate the ability of eq. (4) to determine the hydrodynamic wall location and (b) make a comprehensive comparison between equilibrium and non-equilibrium measurements of slip.

Our simulations were performed using the LAMMPS software [18]. The model system,

simulation setup and parameters as well as our results are described in detail below.

### 3.1 Molecular simulation setup

We consider a system comprising a dense liquid bounded by two fcc-structured walls in a slab geometry. Atomic interactions follow the generalized Lennard-Jones potential [19]

$$u_{ij}(r) = 4\varepsilon_{ij} \left[ \left( \frac{\sigma_{ij}}{r} \right)^{12} - C_{ij} \left( \frac{\sigma_{ij}}{r} \right)^6 \right], \quad (5)$$

where  $r$  denotes the distance between atoms  $i$  and  $j$ .

In what follows, we will use subscript  $s$  to denote solid atoms and their properties and  $l$  to denote liquid atoms and their properties. All quantities will be reported in non-dimensional units using the characteristic time  $\tau_{LJ} = \sqrt{m_l \sigma_{ll}^2 / \varepsilon_{ll}}$ , the characteristic distance  $\sigma_{ll}$  and the potential well depth  $\varepsilon_{ll}$  associated with the liquid-liquid interaction. In all our simulations  $C_{ss} = C_{ll} = 1$ , while  $C_{sl}$  was varied in the range  $0.4 \leq C_{sl} \leq 1$  as will be discussed below.

The simulated system measured 30.8 LJ units in each of the two dimensions parallel to the walls; the distance between the walls was also  $L = 30.8$  units; increasing  $L$  to 61.6 units did not produce any significant change in our results.

Each wall consisted of a 7.71 unit thick FCC slab of atoms divided into three regions, each under different dynamics. The outermost region contained three atomic layers frozen in place. The middle region contained 7 atomic layers thermostated to the desired system temperature ( $T$ ) via a Nosé–Hoover thermostat. The innermost region, in contact with the fluid, comprised of a single atomic layer under NVE dynamics. The surface of the wall exposed to the fluid is the (0,0,1) plane of the FCC crystal. The wall density was fixed at  $n_w=1.09$ . In all simulations  $m_s = 5$  ( $m_l = 1$ ),  $\sigma_{sl} = 1$  ( $\sigma_{ll} = 1$ ) and  $\varepsilon_{ss} = 4$  ( $\varepsilon_{ll} = 1$ ). A potential cutoff of 5 LJ units was used.

#### 3.1.1 Equilibrium simulations

We calculate  $\beta_{GK}$  by numerical integration of the wall-force autocorrelation trace, namely inserting the result for  $\int_0^\infty \langle F_x(t) F_x(0) \rangle dt$  into (2). In all results presented here, the "plateau" value of  $\int_0^\infty \langle F_x(t) F_x(0) \rangle dt$  was identified with the maximum value of this function, in accordance with our discussion in section 2.

#### 3.1.2 Non-equilibrium simulations

We performed Couette flow simulations at wall speeds of  $\pm 0.1$ , which are sufficiently small for non-linear effects to be negligible and viscous heating to be small (maximum temperature variation across the fluid was less than 0.01). The non-equilibrium slip length, denoted

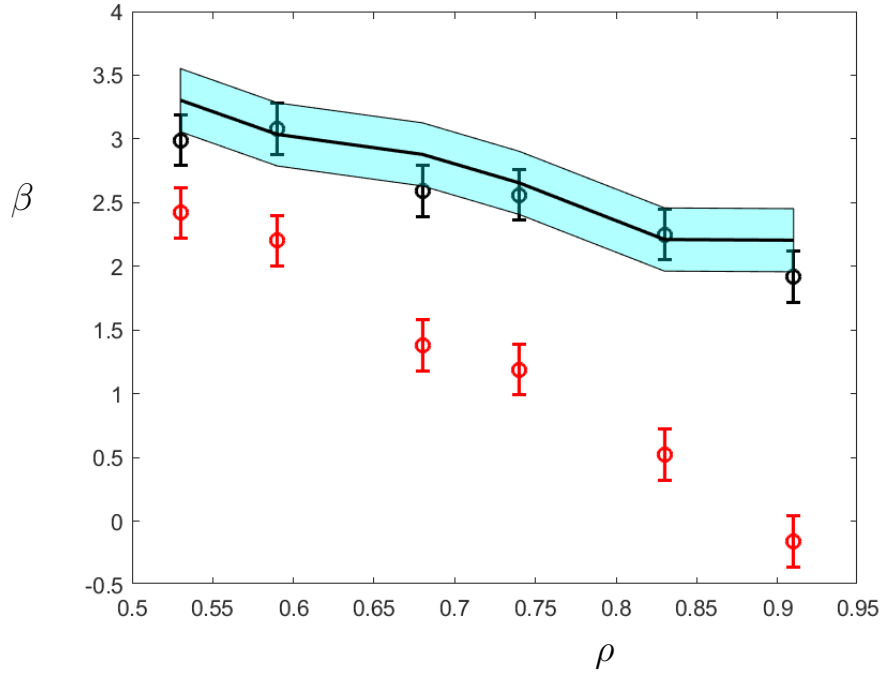


Figure 2: Comparison between the Green-Kubo prediction,  $\beta_{GK}$ , and the non-equilibrium slip,  $\beta_{neq}$ , as a function of fluid density at  $T = 1.5$  with  $\varepsilon_{sl} = 1$  and  $C_{sl} = 0.6$ . Red symbols denote  $\beta_{neq}$  at  $z = 0$ , black symbols denote  $\beta_{neq}$  referred to  $z = z_{GK}^w$  ( $\beta_{neq} + z_{GK}^w$ ), while the predictions and uncertainty associated with  $\beta_{GK}$  are shown by the black line and blue shading, respectively.

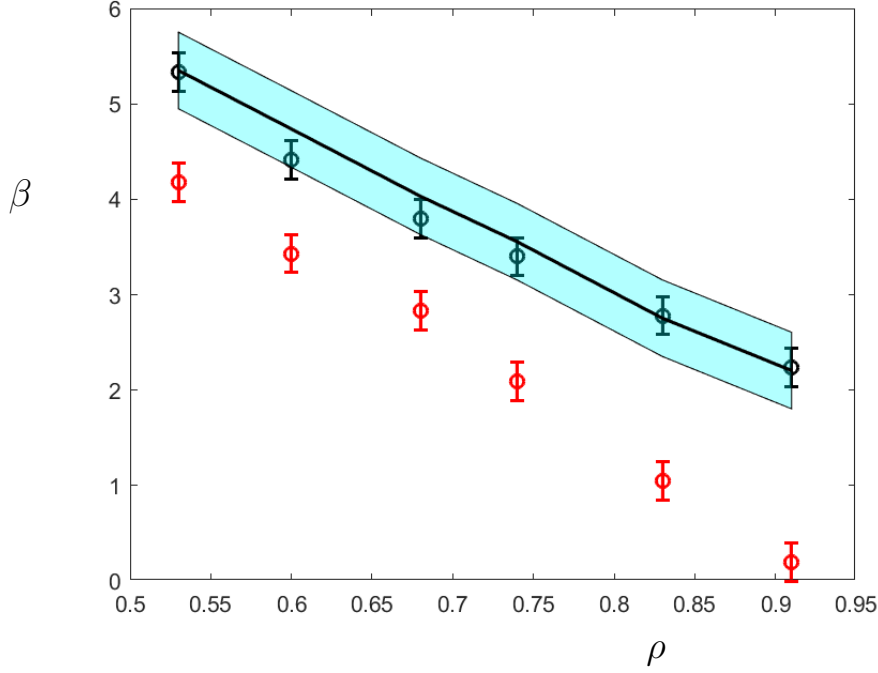


Figure 3: Comparison between the Green-Kubo prediction,  $\beta_{GK}$ , and the non-equilibrium slip,  $\beta_{neq}$ , as a function of fluid density at  $T = 1.5$  with  $\varepsilon_{sl} = 0.6$  and  $C_{sl} = 0.6$ . Red symbols denote  $\beta_{neq}$  at  $z = 0$ , black symbols denote  $\beta_{neq}$  referred to  $z = z_{GK}^w$  ( $\beta_{neq} + z_{GK}^w$ ), while the predictions and uncertainty associated with  $\beta_{GK}$  are shown by the black line and blue shading, respectively.

by  $\beta_{neq}$  was defined as the distance into the wall at which the extrapolated fluid velocity profile reaches the wall speed value. The above extrapolation was performed via a linear approximation of the velocity profile fitted over the middle 75 % of the fluid domain, away from the layering present close to the walls [20].

Here we note that the slip length obtained by this procedure implicitly assumes that the hydrodynamic wall location is  $z = 0$  ( $z_{neq}^w = 0$ ). As will be seen below, this leads to considerable differences between the equilibrium and non-equilibrium results for the slip length. The two can be compared by referring both to the same hydrodynamic wall location. In the present case, this was done by referring the non-equilibrium value to the GK hydrodynamic wall location, or in other words, by comparing  $\beta_{GK}$  to  $\beta_{neq} + z_{GK}^w$ , where  $z_{GK}^w$  was determined by applying eq. (4) to the non-equilibrium MD data. We note that due to the linear velocity profile in Couette flow, this convention is arbitrary: comparing  $\beta_{GK} - z_{GK}^w$  to  $\beta_{neq}$  is equivalent.

### 3.2 Simulation results

Simulations were performed for a wide variety of conditions, including variable liquid density, variable temperature, variable solid-liquid attraction as characterized by  $C_{sl}$  and variable



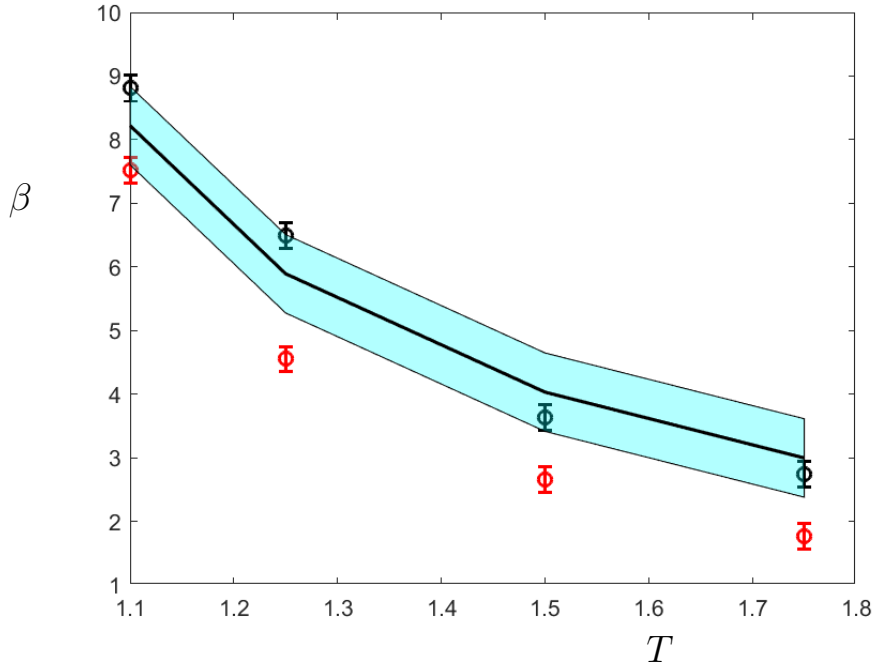


Figure 4: Comparison between the Green-Kubo prediction,  $\beta_{GK}$ , and the non-equilibrium slip,  $\beta_{neq}$ , as a function of temperature at  $\rho = 0.68$  with  $\varepsilon_{sl} = 0.6$  and  $C_{sl} = 0.6$ . Red symbols denote  $\beta_{neq}$  at  $z = 0$ , black symbols denote  $\beta_{neq}$  referred to  $z = z_{GK}^w$  ( $\beta_{neq} + z_{GK}^w$ ), while the predictions and uncertainty associated with  $\beta_{GK}$  are shown by the black line and blue shading, respectively.

liquid-solid interaction strength. Figures (2)-(6) show comparisons between the slip length as determined from eq. (2) via equilibrium simulations ( $\beta_{GK}$ ), the slip length as determined by non-equilibrium simulations ( $\beta_{neq}$ ) and the non-equilibrium slip length referred to  $z = z_{GK}^w$  ( $\beta_{neq} + z_{GK}^w$ ). Each datapoint corresponds to the average value of the results from each of the two walls in the system. In these comparisons, eq. (2) was evaluated using bulk fluid properties.

The results clearly establish that non-equilibrium measurements of the slip length at the fluid-solid interface, that is without taking into account the hydrodynamic wall location, can be very different from those predicted by the GK theory (2). However, when the hydrodynamic wall location is taken into account, in the present figures by referring the non-equilibrium result to this location, the agreement between the two methods is excellent. This also serves as a validation of using (4) to determine the hydrodynamic wall location.

These results also show that the magnitude of  $z_{GK}^w$  can be significantly larger than the value of one LJ unit usually assumed in the literature and as such it cannot be neglected, especially since it appears to be sensitive to the fluid state.

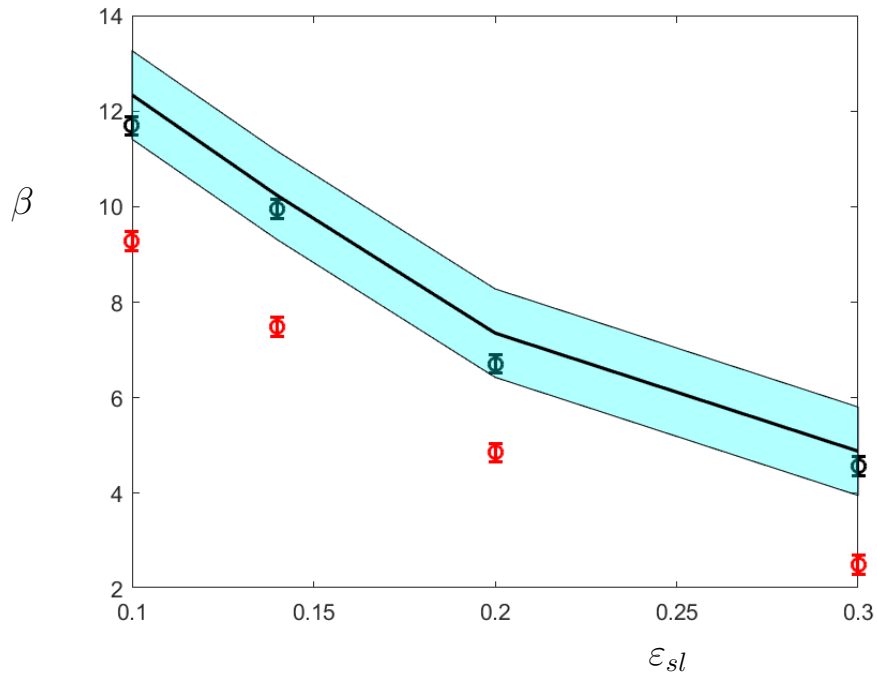


Figure 5: Comparison between the Green-Kubo prediction,  $\beta_{GK}$ , and the non-equilibrium slip,  $\beta_{neq}$ , as a function of  $\varepsilon_{sl}$  at  $T = 0.825$  and  $\rho = 0.83$  with  $C_{sl} = 1$ . Red symbols denote  $\beta_{neq}$  at  $z = 0$ , black symbols denote  $\beta_{neq}$  referred to  $z = z_{GK}^w$  ( $\beta_{neq} + z_{GK}^w$ ), while the predictions and uncertainty associated with  $\beta_{GK}$  are shown by the black line and blue shading, respectively.

## 4 An expression for $\beta$ which does not involve a GK integral

In this section we discuss a model for calculating  $\beta$  without evaluating a GK integral. This result is inspired by previous work [6] where such an expression was developed by relating the force autocorrelation integral in (2) to a model for the relaxation dynamics of the density-density correlation function, using a number of approximations as well as a detailed account of fluid-solid interaction dynamics. The present work also models the force autocorrelation integral but follows a different route, based on the observation, first reported for the case of the Kapitza resistance [21], that the timescale associated with the GK integral governing interfacial transport can be approximately estimated using bulk fluid transport properties. This observation enables the elimination of the autocorrelation integral in terms of the mean square of the tangential component of the wall-fluid force and known *fluid properties*, arguably resulting in a simpler and more physically intuitive final expression.

Following [21] we write (2) in the form

$$\beta = \frac{\mu A k_B T}{\langle F_x^2 \rangle \int_0^\infty \phi(t) dt} = \frac{\mu A k_B T}{\langle F_x^2 \rangle I_\beta} \quad (6)$$

where  $\phi(t) = \langle F_x(t) F_x(0) \rangle / \langle F_x^2 \rangle$  and

$$I_\beta = \lim_{t \rightarrow \infty} \int_0^t \phi(t') dt' \quad (7)$$

The importance of this rearrangement is that it reduces the contribution of the GK integral in (2) into the two distinct factors, namely  $\langle F_x^2 \rangle$ , which is strongly dependent on the fluid-solid interaction and fluid state, and the timescale  $I_\beta$  which our MD simulations show, in agreement with the results in [21] for the case of the Kapitza resistance, is a very weak function of the fluid state and fluid-solid interaction.

Further progress can be made by introducing the assumption  $I_\beta = \tau / D_\beta$ , where  $D_\beta$  is a constant and  $\tau$  is the *homogeneous* fluid viscous relaxation timescale defined by

$$\mu = \frac{1}{V k_B T} \int_0^\infty \langle \Pi_{ij}(t) \Pi_{ij}(0) \rangle dt = \frac{\langle \Pi_{ij}^2 \rangle}{V k_B T} \int_0^\infty \frac{\langle \Pi_{ij}(t) \Pi_{ij}(0) \rangle}{\langle \Pi_{ij}^2 \rangle} dt = G_\infty \tau \quad (8)$$

where  $\Pi_{ij}$  denotes a non-diagonal component of the *homogeneous* fluid stress tensor ( $i \neq j$ ) and

$$G_\infty = \frac{1}{V k_B T} \langle \Pi_{ij}^2 \rangle \quad (9)$$

is the fluid high-frequency shear modulus [22]. This assumption yields

$$\beta = \frac{D_\beta G_\infty k_B T}{A^{-1} \langle F_x^2 \rangle} \quad (10)$$

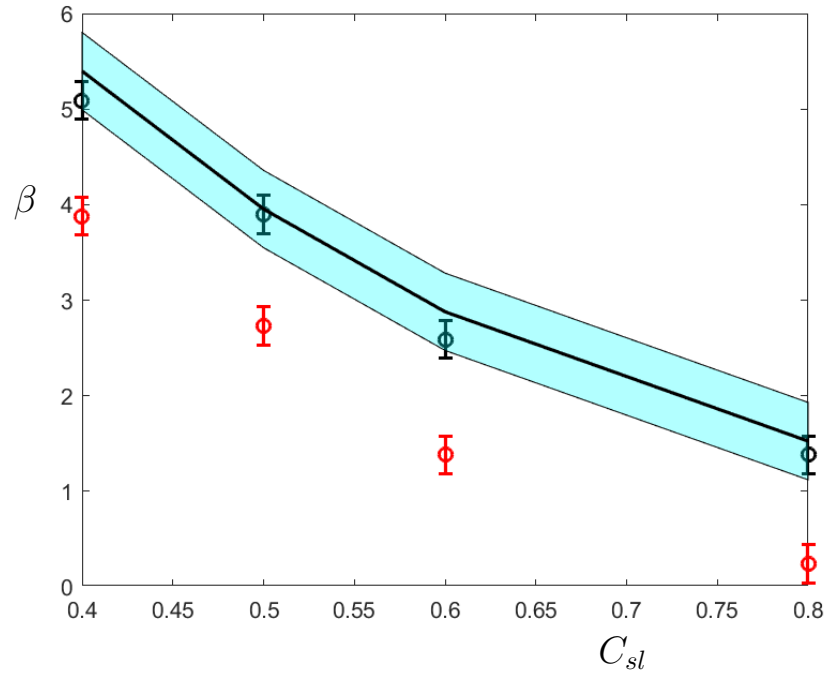


Figure 6: Comparison between the Green-Kubo prediction,  $\beta_{GK}$ , and the non-equilibrium slip,  $\beta_{neq}$ , as a function of  $C_{sl}$  at  $T = 1.5$  and  $\rho = 0.68$  with  $\varepsilon_{sl} = 1$ . Red symbols denote  $\beta_{neq}$  at  $z = 0$ , blue symbols denote  $\beta_{neq}$  referred to  $z = z_{GK}^w$  ( $\beta_{neq} + z_{GK}^w$ ), while the predictions and uncertainty associated with  $\beta_{GK}$  are shown by the black line and blue shading, respectively.

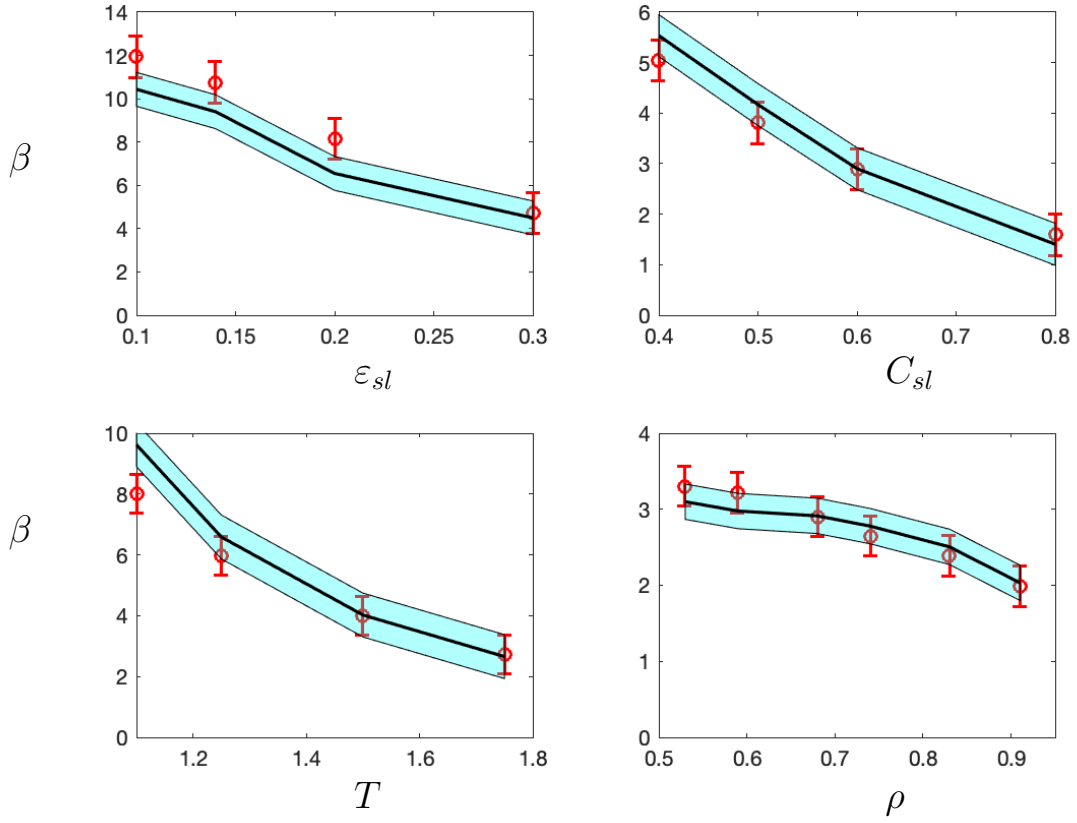


Figure 7: Validation of relation (10) for a variety of conditions. MD simulation results and associated uncertainty (for  $\beta_{GK}$ ) are shown in red symbols, while the prediction of equation (10) and associated uncertainty are denoted by the black line and blue shading, respectively. Simulations performed at the following conditions: Top left,  $T = 1.5, C_{sl} = 1, \rho = 0.83$ ; top right,  $T = 1.5, \varepsilon_{sl} = 1, \rho = 0.68$ ; bottom left,  $\varepsilon_{sl} = 0.6, C_{sl} = 0.6, \rho = 0.68$ ; bottom right,  $T = 1.5, \varepsilon_{sl} = 1, C_{sl} = 0.6$ .

in which the dynamics "hidden" within the GK integral have been expressed in terms of system properties.

Figure (7) shows that eq (10) provides a very reasonable approximation to our MD results. In this comparison, the value  $D_\beta = 1.05$  was chosen as the one that gives best overall agreement between expression (10) and the MD results;  $G_\infty$  was calculated using the analytical expression for a LJ potential in [23], while  $A^{-1}\langle F_x^2 \rangle$  was taken from MD simulations. Here we emphasize that once determined as described above, the value of  $D_\beta$  is not adjusted in any way; this is quite remarkable given the variety of fluid conditions and solid-liquid interaction parameters explored in this figure.

## 5 Discussion

We have shown that non-equilibrium and equilibrium measurements of slip are consistent, provided the hydrodynamic wall location associated with the equilibrium measurement is taken into account. Moreover, our simulations show that the hydrodynamic wall location

associated with  $\beta_{GK}$  is dependent on the fluid state in a non-trivial manner and can be a significant fraction of the slip length. In other words,  $z_{GK}^w$  cannot be neglected in general; instead, a reliable method for its calculation is needed. Our work has shown that reliable and accurate measurements of  $z_{GK}^w$  can be obtained by utilizing the tangential force balance at the wall in a non-equilibrium shear flow, given by equation (4). Given that this latter approach requires a non-equilibrium simulation, we note here that a method which uses MD simulations of two non-equilibrium flows, namely a Couette and a Poiseuille flow, to calculate the slip length and the associated hydrodynamic wall location was recently proposed in [24]. The need for two distinct simulations for simultaneously determining both of these quantities was first discussed in [5]; a variant of this approach was implemented for dissipative particle dynamics simulations in [25]. A comparison between the method proposed here and the one that uses 2 non-equilibrium simulations would be an interesting topic for future work.

The relative success of the approximation  $I_\beta = \tau/D_\beta$  is also worth noting, both because it enables the closed form expression (10), but also because the similar success of the analogous approximation in the case of the Kapitza resistance [21] suggests some generality. Models such as eq. (10) as well as others [6, 9] are valuable because they replace the GK integral with a more transparent connection between system properties and the slip length. Returning to model (10), further work is required for developing methodologies for calculating the value of  $D_\beta$  from first principles. We also note that based on our results, model (10) would benefit from a model for predicting the associated hydrodynamic wall location; this will be the subject of future work.

The new GK formulation by Español and collaborators [12, 13], aimed at alleviating the GK plateau issue discussed in section 2, also introduces a modified hydrodynamic wall location  $z_{GK}^{w,C} = z_{GK}^w - G\beta_{GK}/\mu$ , where  $G > 0$ , given in terms of a GK integral, represents a correction to the fluid viscosity at this location due to the wall presence [26]. Provided that the evaluation of  $G$  is less challenging than that of  $z_{GK}^w$ , this new formulation may indeed be preferable, since it could provide less ambiguous estimates of  $\beta_{GK}$  coupled to a smaller in magnitude, and thus less important compared to the slip value, hydrodynamic wall location. Such a formulation would also be advantageous for models such as the one presented in section 4, since it diminishes the importance of accurately determining  $z_{GK}^{w,C}$  (or  $z_{GK}^w$ ).

## 6 Acknowledgements

This material is based upon work supported by the Department of Energy, National Nuclear Security Administration under Award Number DE-NA0003965. The authors would like to thank Professor Pep Español for many helpful discussions.

## References

- [1] Y. Sone. *Molecular Gas Dynamics: Theory, Techniques, and applications*. Birkhauser, 2007.
- [2] N.G. Hadjiconstantinou. “The limits of Navier-Stokes theory and kinetic extensions for describing small-scale gaseous hydrodynamics”. In: *Phys. Fluids* 18 (2006), p. 111301.
- [3] N. Kavokine, R.R. Netz, and L. Bocquet. “Fluids at the nanoscale: From continuum to subcontinuum transport”. In: *Annu. Rev. Fluid Mech.* 53 (2021), pp. 377–410.
- [4] P. A. Thompson and S. M. Troian. “A general boundary condition for liquid flow at solid surfaces”. In: *Nature* 389.6649 (1997), pp. 360–362.
- [5] L. Bocquet and J.-L. Barrat. “Hydrodynamic boundary conditions, correlation functions, and Kubo relations for confined fluids”. In: *Phys. Rev. E* 49 (1994), pp. 3079–3092.
- [6] J.L. Barrat and L. Bocquet. “Influence of wetting properties on hydrodynamic boundary conditions at a fluid/solid interface”. In: *Faraday Discussions* 112 (1999), p. 119.
- [7] S. Lichter, A. Roxin, and S. Mandre. “Mechanisms for Liquid Slip at Solid Surfaces”. In: *Physical Review Letters* 93 (2004), p. 086001.
- [8] A. Martini et al. “Molecular Mechanisms of Liquid Slip”. In: *J. Fluid Mech.* 600 (2008), pp. 257–269.
- [9] N.V. Priezjev and S.M. Troian. “Influence of periodic wall roughness on the slip behavior at liquid/solid interfaces: Molecular scale simulations versus continuum predictions”. In: *Journal of Fluid Mechanics* 554 (2006), p. 25.
- [10] G. J. Wang and N.G. Hadjiconstantinou. “A universal molecular-kinetic scaling relation for slip of a simple fluid at a solid boundary”. In: *Phys. Rev. Fluids* 4 (2019), p. 064291.
- [11] N.G. Hadjiconstantinou. “An atomistic model for the Navier slip condition”. In: *J. Fluid Mech.* 912 (2021), A26.
- [12] D. Duque-Zumajo et al. “Discrete hydrodynamics near solid walls: Non-Markovian effects and the slip boundary condition”. In: *Phys. Rev. E* 100 (2019), p. 062133.
- [13] D. Camargo et al. “Boundary conditions derived from a microscopic theory of hydrodynamics near solids”. In: *J. Chem. Phys.* 150 (2019), p. 144104.
- [14] J.A. de la Torre et al. “Microscopic slip boundary conditions in unsteady fluid flows”. In: *Phys. Rev. Lett.* 123 (2019), p. 264501.
- [15] J.S. Hansen, B.D. Todd, and P. J. Daivis. “Prediction of fluid velocity slip at solid surfaces”. In: *Phys. Rev. E* 84 (2011), p. 016313.
- [16] N. G. Hadjiconstantinou et al. “Statistical error in particle simulations of hydrodynamic phenomena”. In: *J. Comp. Phys.* 187 (2003), pp. 274–297.
- [17] H. Oga et al. “Green-Kubo measurement of liquid-solid friction in finite-size systems”. In: *J. Chem. Phys.* 151 (2019), p. 054502.
- [18] S. Plimpton. “Fast parallel algorithms for short-range molecular dynamics”. In: *J. Comp. Phys.* 117 (1995), pp. 1–19.
- [19] S. Alosious et al. “Prediction of Kapitza resistance at fluid-solid interfaces”. In: *J. Chem. Phys.* 151 (2019), p. 194502.

- [20] G. J. Wang and N.G. Hadjiconstantinou. “Molecular mechanics and structure of the fluid-solid interface in simple fluids”. In: *Phys. Rev. Fluids* 2 (2017), p. 094201.
- [21] N.G. Hadjiconstantinou and M.M. Swisher. “An atomistic model for the thermal resistance of a fluid-solid interface”. In: *J. Fluid Mech.* 934 (2022), R2.
- [22] D. M. Heyes et al. “Transport coefficients of the Lennard-Jones fluid close to the freezing line”. In: *J. Chem. Phys.* 151 (2019), p. 204502.
- [23] R. Zwanzig and R.D. Mountain. “High-Frequency Elastic Moduli of Simple Fluids”. In: *J. Chem. Phys.* 43 (1965), pp. 4464–4471.
- [24] H. Nakano and S. Sasa. “Equilibrium measurement method of slip length based on fluctuating hydrodynamics”. In: *Phys. Rev. E* 101 (2020), p. 033109.
- [25] J. Smiatek, M.P. Allen, and F. Schmid. “Tunable-slip boundaries for coarse-grained simulations of fluid flow”. In: *Eur. Phys. J. E* 26 (2008), pp. 115–122.
- [26] P. Espanol. *Private communication*.